The Region Adjacent to the Highly Immunogenic Site and Shielded by the Middle Domain Is Responsible for Self-Oligomerization/Client Binding of the HSP90 Molecular Chaperone†

Takayuki K. Nemoto,*,‡ Yutaka Fukuma,‡ Shin-ichi Yamada,§ Takeshi Kobayakawa,‡ Toshio Ono,‡ and Yuko Ohara-Nemoto||

Division of Oral Molecular Biology and Division of Oral and Maxillofacial Surgery, Department of Developmental and Reconstructive Medicine, Course of Medical and Dental Sciences, Nagasaki University Graduate School of Biomedical Sciences, 1-7-1 Sakamoto, Nagasaki 852-8588, Japan, and Department of Oral Microbiology, Iwate Medical University School of Dentistry, 1-3-27 Chuodori, Morioka 020-8505, Japan

Received December 12, 2003; Revised Manuscript Received March 23, 2004

ABSTRACT: We here investigated the mechanism of self-oligomerization of the 90-kDa heat shock protein (HSP90) molecular chaperone, because it is known that this oligomerization reflects the client-binding activity. The transition temperatures for the self-oligomerization of the full-length forms of human HSP90α and HtpG (bacterial HSP90), i.e., 45 and 60 °C, respectively, were identical to those for the dissociation of the recombinant N domain (residues 1−400 of human HSP90α and residues 1−336 of HtpG in our definition) from the remainder of the molecule. The N domain of human HSP90α expressed in *Escherichia coli* was oligomeric, and the oligomerization activity was localized within residues 311−350, i.e., C-terminally adjacent to the highly immunogenic site (residues 291−304). Particularly, residues 341−350 were critical on oligomerization. On the other hand, residues 289−389 were indispensable for the interaction with the M domain (residues 401−618) of the molecule. Oligomer formation of the N domain was efficiently suppressed by its extension until Lys546, i.e., residues 401−546, which is required for the interaction with the N domain. Among highly conserved amino acids at residues 289−400, Trp297, Pro379, and Phe384 were essential for the interaction with the M domain. With these observations taken together, we propose as the activation mechanism of HSP90 molecular chaperone that heat stress induces the liberation of the oligomerization/client-binding site of residues 311−350 by disrupting the intramolecular interaction between residues 289−389 and 401−546.

The 90-kDa heat shock protein (HSP90)[1] is either transiently or stably associated with various but specific client proteins that are unstable unless chaperoned with HSP90. HSP90 generally functions in cooperation with other molecular chaperones and cochaperones. Yonehara et al. (*1*) reported that the molecular chaperone activity of mammalian HSP90 was activated at temperatures higher than 46 °C in vitro and that the purified form of HSP90 became self-oligomerized under these conditions (*1*). Thus, self-oligomerization of HSP90 seems to be mediated by the binding with each other of HSP90 molecules via the client-binding site (*1*). In fact, the binding of *Escherichia coli* HtpG to glutathione *S*-transferase (GST), a model client protein, was also activated at elevated temperatures, and the oligomerization of *E. coli* HtpG occurred at these temperatures (*2*). These studies indicate that heat-induced activation is generally observed on the HSP90-family molecular chaperones.

Various regions of HSP90 have been proposed to be involved in its interactions with target proteins. For instance, a highly charged region of chick HSP90α (amino acids 221−290) is essential for the binding to estrogen and mineralocorticoid receptors (*3*), and this region is also involved in the binding to the α subunit of casein kinase CK2 (*4*). However, the corresponding highly charged region of yeast HSP82 (residues 223−289) is dispensable for its viability and function in yeast (*5*). Deletion experiments on HSP90*β* demonstrated that amino acids 327−340, which are proximal to the highly charged region, are essential for chaperoning of serine/threonine kinase Akt/PKB (*6*). However, it should be carefully interpreted as to whether these proposed regions directly associate with client proteins or whether their loss abrogates the interaction as a consequence of loss of some other functions. On the basis of the three-dimensional structure of the M domain (residues 273−516) of yeast

† This work was supported by grants from the programs Grants-in-Aid for Scientific Research on Priority Areas from the Ministry of Education, Science, Sports, and Culture of Japan (to T.K.N.) and Grants-in Aid for Scientific Research (C) from the Japan Society for the Promotion of Science (to T.K.).

* To whom correspondence should be addressed. Tel: 81 95 849 7640. Fax: 81 95 849 7642. E-mail: tnemoto@net.nagasaki-u.ac.jp.

‡ Division of Oral Molecular Biology, Nagasaki University Graduate School of Biomedical Sciences.

§ Division of Oral and Maxillofacial Surgery, Nagasaki University Graduate School of Biomedical Sciences.

|| Department of Oral Microbiology, Iwate Medical University School of Dentistry.

[1] Abbreviations: HSP90, 90-kDa heat shock protein; HSP90α and HSP90*β*, α and *β* isoforms of HSP90, respectively; HSP82, yeast 82-kDa heat shock protein; HtpG, *Escherichia coli* homologue of mammalian HSP90; H_6HSP90α and H_6HtpG, HSP90α and HtpG tagged with a histidine hexamer at the N-terminus, respectively; GST, glutathione *S*-transferase; mAb, monoclonal antibody; PAGE, polyacrylamide gel electrophoresis; SDS, sodium dodecyl sulfate.

10.1021/bi036235f CCC: $27.50
Published on Web 05/18/2004

HSP82, Beyer et al. (*7*) proposed that residues 327−340, equivalent to residues 347−360 of human HSP90α, possess an amphipathic structure and potentially bind to a client protein.

Another approach using model client proteins has been employed to clarify the client-binding sites of HSP90. When citrate synthase and insulin were used as client proteins, mammalian HSP90 was found to possess two distinct client-binding sites (*8*, *9*): one of them was located in the N-terminal 210 amino acids, and its activity was modulated by ATP and geldanamycin, a specific inhibitor of HSP90 molecular chaperone; and the other was in the C domain. Minami et al. (*10*) confirmed the existence of respective client-binding sites in the N and C domains. Similarly, the C-terminal fragment (residues 494−782) of human 94-kDa glucose-regulated protein protects the catalytic subunit of protein kinase CK2 against thermal aggregation (*11*). Interestingly, we recognized only a single client-binding site in *E. coli* HtpG, which was solely localized in the N domain (residues 1−336) of this 624 amino acid protein (*12*). Amino acid substitution of human HSP90α revealed that the hydrophobic segment (residues 662−678) of the C domain was essential for both dimer formation and the client-binding activity (*13*). Thus, at present, the client-binding activity of the C domain is indistinguishable from the dimer-forming interaction of HSP90 (*13*). Thus, it seems necessary to further investigate whether the site at the C-terminal side is truly involved in the client binding under physiological conditions. In contrast, the client-binding site at the N-terminal side should be directly involved in the function of the molecular chaperone, although its precise location is still obscure.

In the present study, we investigated the mechanism on self-oligomerization of the HSP90 molecular chaperone in order to elucidate the N-terminal client-binding site and the mechanism of the heat-induced activation of the client-binding activity. We demonstrate herein that amino acids 311−350, which are C-terminally proximal to the highly immunogenic site (residues 291−304) of HSP90 (*14*), are responsible for the self-oligomerization. We propose that the heat-induced liberation of residues 289−389 from residues 401−546 triggers the self-oligomerization and, presumably, client binding as well.

EXPERIMENTAL PROCEDURES

Materials. The following materials were used: expression vector pQE9 and plasmid pREP4 from Queen Inc. (Chatsworth, CA); pTrcHis-TOPO from Invitrogen (Carlsbad, CA); pGEX4T-1, glutathione Sepharose, and low-molecular-weight markers from Amersham Biosciences (Piscataway, NJ); restriction enzymes and DNA-modifying enzymes from Nippon Gene (Tokyo, Japan); the kaleidoscope prestained molecular standard from Bio-Rad (Richmond, CA); Talon metal affinity resin from Clontech Laboratories Inc. (Palo Alto, CA); trypsin (5200 USP units/mg of protein) and N^{α}-acetyl-L-tosyl-L-phenylalanine chloromethyl ketone from Sigma (St. Louis, MO); alkaline phosphatase-conjugated goat anti-mouse IgG from EY Laboratories Inc. (San Mateo, CA); and rabbit anti-mouse Ig(G + A + M) from Zymed Laboratories Inc. (San Francisco, CA). Anti-human HSP90 monoclonal antibodies (mAbs), K41102, K41110, and K41218, were prepared as reported previously *(14)*. Bacterial strain BTH101 [F^-, *cya-99*, *araD139*, *galE15*, *galK16*, *rpsL1*(*Str*^{r}), *hsdR2*, *mcrA1*, *mcrB1*] and plasmids pKT25^{kan} and pUT18C^{amp} were generously provided by Dr. L. Selig (Hybrigenics, S. A., Paris, France). All other reagents were of analytical grade.

Definition of Domains. According to our previous results on limited proteolysis and regional interactions, we could divide human HSP90α as well as *E. coli* HtpG into three domains. Amino acid residues 1−400, 401−618, and 619−732 of human HSP90α (*14*, *15*) and 1−336, 337−552, and 553−624 of *E. coli* HtpG correspond to the N, M, and C domains (*16*), respectively (see Figure 1a). The domain border between the N and M domains is distinct from that defined by Stebbins et al. (*17*) and Prodromou et al. (*18*). Our definition of the N domain is based on the cleavage site most susceptible to limited proteolysis (*14*−*16*), whereas the others define the N-terminal core region (residues 1−220/230) as that highly resistant to proteolysis (*17*, *18*). In the present study, truncated forms of the two HSP90 species were expressed mainly on the basis of domain units, which were referred to as N, M, and MC for the N domain, M domain, and MC domain, respectively. In the case of other regions being expressed, we added the number of amino acid residues such as 1−521 and 1−400/421−560.

Construction of Bacterial Expression Vectors. The DNAs encoding the full-length form of human HSP90α (*19*) and *E. coli* HtpG (*20*) were generously provided by Drs. K. Yokoyama (Riken Life Science Center, Tsukuba, Japan) and E. A. Craig (University of Wisconsin Medical School, Madison, WI), respectively. Construction of the pQE9 plasmid (Qiagen) encoding the domains of HSP90α and HtpG and residues 1−312 of HSP90α tagged with a histidine hexamer was described previously (*2*, *21*). Y1090[pREP4] was transformed with constructs and selected on Luria broth agar plates containing 50 μg/mL ampicillin and 25 μg/mL kanamycin. For expression of amino acids 1−320, 1−330, 1−340, 1−350, 1−360, 1−372, 1−386, 1−389, 1−521, 1−541, 1−546, 1−560, and 289−400 of human HSP90α, DNA fragments encoding these regions were amplified by PCR and then directly inserted into the pTrcHis-TOPO TA cloning vector (Invitrogen) in-frame according to the manufacturer's recommendation. For expression of residues 1−400/421−560 and 1−400/561−560, DNA fragments encoding the corresponding regions of HSP90α were amplified together with the plasmid DNA by High Fidelity PCR (Roche, Mannheim, Germany) with appropriate primers that introduced the intended deletions. *E. coli* TOP-10 was transformed with these PCR products following digestion of the template DNA by *Dpn*I. Amino acids 289−372 and 311−372 were expressed as glutathione *S*-transferase (GST) fusion proteins by insertion of the appropriate PCR products in pGEX4T-1 (*14*). The DNA insertion was confirmed by Hot Star PCR (Qiagen Inc., Chatsworth, CA), and mutations were confirmed by DNA sequencing (ABI PRISM 310, PE Applied Biosystems).

Bacterial Two-Hybrid System. The intramolecular interaction between the N and M domains was examined by using the bacterial two-hybrid system according to the method of Karimova et al. (*22*) as described previously (*12*). Construction of pKT25^{kan}-HSP90α 1−320, 1−372, and 1−400 (N domain) and pKT25^{kan}-HtpG 1−336 (N domain) and that of pUT18C^{amp}-HSP90α 401−732 (MC domain) and HtpG 337−624 (MC domain) were described previously (*23*).

Similarly, DNA fragments encoding amino acids 1−386 and 1−389 of HSP90α were amplified by PCR and inserted in a *Pst*I/*Bam*HI site of pKT25^{kan}. The apparent complex formation between coexpressed recombinant proteins, i.e., the wild or mutated type of the N domain and the MC domain was distinguished by color development of the colonies on MacConkey indicator media agar plates containing 1% maltose. Quantitative data were obtained by measurement of the β-galactosidase activity that was enhanced by complex formation (*22*, *23*).

Substitution of Amino Acids Conserved within Residues 289−*400*. Eleven amino acids within residues 289−400 of pKT25^{kan}-HSP90α were substituted by Gly or Ala by using PCR-based, site-directed mutagenesis in combination with *Dpn*I degradation for elimination of template DNA. Among them, three amino acids, i.e., Trp297Gly, Pro379Ala, and Phe384Ala, were further mutagenized by using degenerate primers (5′-NNN at the corresponding codons: N = G, A, T, or C). Pro379Ala was also mutagenized with another set of primers (5′-NSN at the codon: S = G or C; N = G, A, T, or C). Eight amino acids and one stop codon could be formed with this primer set. The resulting plasmids, pKT25^{kan}-HSP90α-N-Gly297Xaa, Ala379Xaa, and Ala384Xaa (Xaa, any amino acids), were subjected to the two-hybrid analysis as described above. Mutated amino acids of positive clones that developed red color on MacConkey indicator plates were deduced by DNA sequencing.

Expression and Purification of Recombinant Proteins. Recombinant proteins encoded by the pQE9 and pTrcHis-TOPO vectors were denoted with H_6 as H_6HSP90α, because a histidine hexamer tag was present within the N-terminal 12 and 35 amino acids, respectively, encoded by the two vectors. After cultivation of the transformed bacteria at 37 °C overnight, recombinant proteins were expressed at 30 °C for 5 h in the presence of 0.2 mM isopropyl β-D-thiogalactopyranoside. Recombinant proteins were purified with a Talon affinity column according to the manufacturer's protocol except that 10 mM imidazole was included in the lysis/washing buffer. Bound proteins were eluted with 0.1 M imidazole (pH 8.0) containing 10% (v/v) glycerol. GST-HSP90α 289−372 and 311−372 were expressed as above and purified on a glutathione Sepharose column according to the manufacturer's procedure. Proteins were immediately used for experiments or were stored at −80 °C until used.

Sodium Dodecyl Sulfate−*Polyacrylamide Gel Electrophoresis (SDS*−*PAGE)*. Electrophoresis was performed in the presence of 0.1% SDS at a polyacrylamide concentration of 12.5% unless otherwise stated. Generally, 0.5−1 μg of proteins was loaded onto SDS−PAGE. Separated proteins were stained with Coomassie brilliant blue or subjected to immunoblotting. Low-molecular-weight markers (Amersham) or kaleidoscope markers (Bio-Rad) were used as molecular markers.

Polyacrylamide Gel Electrophoresis under Nondenaturing Conditions. To estimate molecular configurations, recombinant proteins (1−2 μg) or their mixtures were subjected to PAGE on a 7.5% polyacrylamide gel under nondenaturing conditions (*15*). We found that elution buffers, i.e., 0.1 M imidazole (pH 8) containing 10% (v/v) glycerol for H_6-tagged proteins and 40 mM Tris-HCl (pH 8.0) and 10% (v/v) glycerol containing 10 mM glutathione for GST fusion proteins, as well as addition of 5 mM 2-mercaptoethanol and 1 mM dithiothreitol, did not affect the mobility of recombinant proteins and their interactions. Accordingly, purified proteins were directly subjected to PAGE. Electrophoresis was performed at room temperature at a constant voltage of 50 V. Separated proteins were stained with Coomassie brilliant blue or subjected to immunoblotting. Because HSP90 is an acidic protein with an isoelectric point (p*I*) of 5.2 (*24*), we chose ovalbumin (45 kDa, p*I* 4.6), bovine serum albumin (66 kDa as monomer, 132 kDa as dimer, and 198 kDa as trimer, p*I* 4.8), and catalase (240 kDa, p*I* 5.5) with similar p*I*s as references to neutralize the charge effect.

Immunoblotting Analysis. Proteins (0.1−0.5 μg) separated on SDS−PAGE or native PAGE gels were subjected to immunoblotting analysis as described previously (*14*). The epitopes of mAbs K41102 and K41110 were localized at Lys_{247}−Glu_{257} (immunogenic site Ia) and Asn_{291}−Ile_{304} (immunogenic site Ic) of human HSP90α, respectively (*14*). The epitope of K41218 was localized within Leu_{48}−Glu_{196} (*14*) and was further defined to Asp_{71}−Ile_{78} by the Fli-Trix flagellin fusion display system (Invitrogen) (Y. Fukuma and T. K. Nemoto, unpublished observation). According to the class (IgG or IgM) of mAbs used, alkaline phosphatase-conjugated goat anti-mouse IgG or rabbit anti-mouse Ig(G + A + M) was used as the second antibody. First and second antibodies were used at 1−3 and 0.2 μg/mL, respectively. Blots were finally visualized by incubation with 5-bromo-4-chloro-3-indolyl phosphate and nitro blue tetrazolium (Promega, Madison, WI).

Protein Concentration. Protein concentrations were determined by use of the bicinchoninic acid method (Pierce, Rockford, IL).

RESULTS

Temperature-Dependent Changes in the Oligomerization and Domain−*Domain Interaction of HSP90.* The N domain (H_6HSP90α-N and H_6HtpG-N), the M domain of HtpG (H_6-HtpG-M), and the MC domains (H_6HSP90α-MC and H_6-HtpG-MC) were expressed and purified to homogeneity (Figure 1a,b). In contrast to the monomeric nature of H_6-HtpG-N, H_6HSP90α-N existed as oligomers, migrating near the top of a separation gel of PAGE under nondenaturing conditions (Figure 1c, compare lanes 1 and 2). Oligomerization of H_6HSP90α-N was ascertained by its elution at void volume on size-exclusion gel chromatography of Sephacryl S200 (data not shown). We attempted to prepare the monomeric form of H_6HSP90α-N by expressing the recombinant protein at lower temperatures, but it was still oligomeric even when expressed at 20 °C. Immunoblotting analysis indicated that the recombinant protein was already oligomerized in the bacterial lysate prior to the purification step (data not shown).

The N and M domains associated with each other through an intramolecular interaction, and this interaction was even accomplished across the species (Figure 1c, lanes 5−8, and ref *12*). The positions of the complexes on PAGE were comparable between the N domains of human HSP90α and *E. coli* HtpG (Figure 1c, compare lanes 5 and 7 and lanes 6 and 8). These results indicated that, although most H_6-HSP90α-N existed as oligomers, a small portion of these oligomers dissociated into monomers and formed a complex with H_6HtpG-MC and H_6HtpG-M. This also indicates that the site responsible for self-oligomerization is identical or

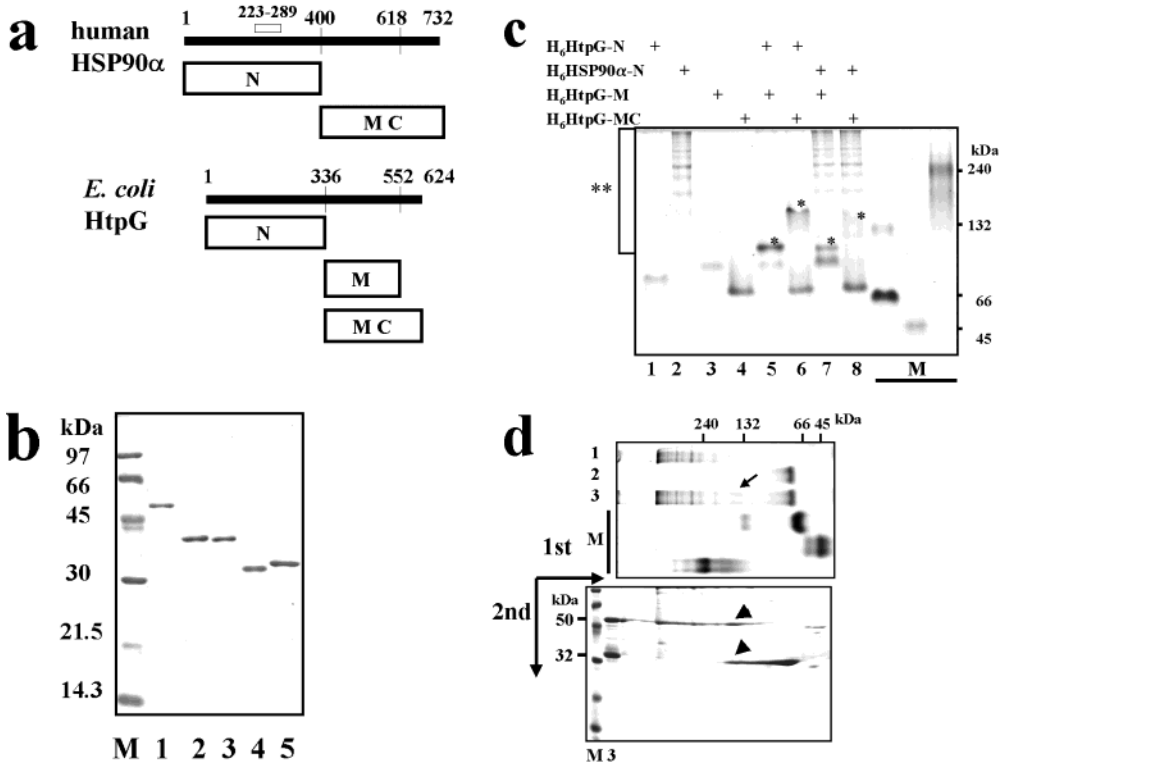

FIGURE 1: Interaction between the N and M domains. (a) Schematic illustration of the three-domain structures of human HSP90α and *E. coli* HtpG and the recombinant domains expressed. Residues 223−289 constitute the highly charged region specific to eukaryotic HSP90. (b) Recombinant proteins were purified and separated on SDS−PAGE. Lanes: 1, H_6HSP90α-N; 2, H_6HSP90α-MC; 3, H_6HtpG-N; 4, H_6HtpG-M; and 5, H_6HtpG-MC. (c) Recombinant proteins in various combinations as indicated on the top were electrophoresed on PAGE gels under nondenaturing conditions. The amount of proteins loaded was 1.5 μg except for H_6HSP90α-N (3 μg). Asterisks represent complexes formed, and double asterisks indicate oligomeric forms. (d) H_6HSP90α-N (lane 1, 4 μg), H_6HtpG-MC (lane 2, 0.5 μg), or their mixture (lane 3) was electrophoresed on the first dimension PAGE under nondenaturing conditions. After the electrophoresis of the mixture (three times of lane 3), proteins were further developed on the second dimension SDS−PAGE. An arrow represents complexes formed. Arrowheads represent the protein constituents of the complexes. Lane M represents molecular markers. Electrophoretic images (panels b and d) are representatives of two separate experiments, and the image of panel c is representative of three separate experiments.

Table 1: Interaction between the N and MC Domains of HSP90 and HtpG[a]

pKT25^{kan}-	pUT18C^{amp}-	activity ± SD (%)
vector	vector	3.6 ± 0.6
HSP90α-N	vector	2.6 ± 0.1
HSP90α-N	HSP90α-MC	84.3 ± 25.1
HtpG-N	vector	3.3 ± 0.7
HtpG-N	HtpG-MC	100.0 ± 19.6
HSP90α-N	HtpG-MC	92.5 ± 4.8
HtpG-N	HSP90α-MC	60.4 ± 21.4

[a] Binding activity of the HtpG-N to HtpG-MC was set at 100%. Values are means ± SD of three independent colonies. Data are representatives of two separate experiments.

at least overlaps that for the domain−domain interaction. The complex between H_6HSP90α-N and H_6HSP90α-MC was not found under these experimental conditions (*14*).

The two-dimensional PAGE, i.e., the first dimension PAGE under the nondenaturing conditions followed by the second dimension SDS−PAGE, directly demonstrated the complex formation between 50-kDa H_6HSP90α-N and 32-kDa H_6HtpG-MC (Figure 1d). Moreover, the bacterial two-hybrid system demonstrated that the complex was efficiently formed in any combinations of the domains of HSP90α and HtpG (Table 1). This high efficiency may be explained by the property of the two-hydrid system, in which recombinant proteins were coexpressed, and hence, the domain−domain interaction could proceed before the self-oligomerization.

We then compared the heat stability of the N domain and of its complex with the MC domain. When heated at various temperatures for 10 min, H_6HSP90α-N consistently migrated as oligomers with various molecular masses (Figure 2a). In contrast, H_6HtpG-N existed as a monomer and converted to oligomers on exposure to temperatures of 60 °C and higher for 10 min (Figure 2b). The hybrid complex between H_6-HSP90α-N and H_6HtpG-MC was labile at temperatures higher than 45 °C (Figure 2c); and that between H_6HtpG-N and H_6HtpG-MC, at temperatures higher than 60 °C (Figure 2d). Interestingly, the temperature required for the transition to oligomers of H_6HtpG-N was identical to that for dissociation of the H_6HtpG-N−H_6HtpG-MC complex and was also comparable to the transition temperature for oligomerization of the full-length form of HtpG reported previously (*2*). Similarly, the full-length forms of mouse (*1*) and human HSP90 (*2*) converted to oligomeric forms at temperatures higher than 45 °C, which also corresponds to the temperature inducing the dissociation of the HSP90α-N−HtpG-MC complex. Therefore, heat-induced oligomerization of the HSP90-family members was tightly coupled with the disruption of the intradomain interaction between the N and M domains. In this series of experiments we used H_6HtpG-MC as the partner for complex formation, because H_6HSP90α-MC itself has client-binding activity and is therefore self-oligomerized (*13*).

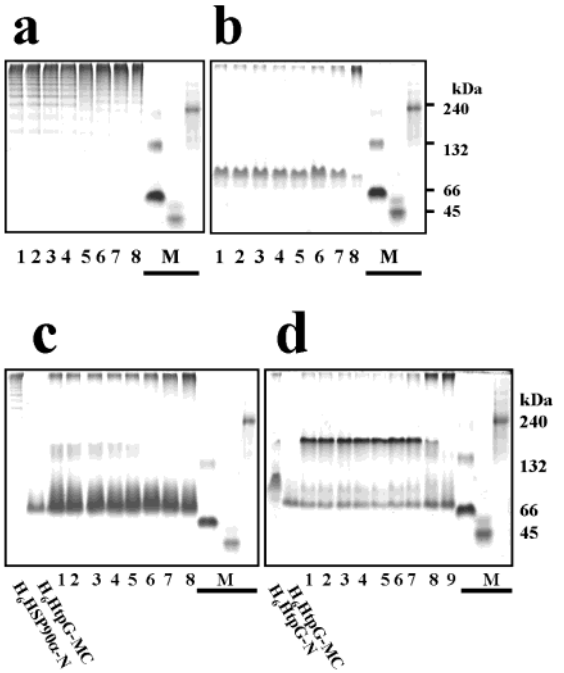

FIGURE 2: Stability of the N-MC complex at elevated temperatures. (a) H_6HSP90α-N (3 μg), (b) H_6HtpG-N (2 μg), (c) a mixture of H_6HSP90α-N (3 μg) and H_6HtpG-MC (2 μg), or (d) a mixture of H_6HtpG-N (1.5 μg) and H_6HtpG-MC (2 μg) was exposed at various temperatures for 10 min. After having been cooled, they were subjected to PAGE under nondenaturing conditions. Lanes: 1, 0 °C; 2, 30 °C; 3, 35 °C; 4, 40 °C; 5, 45 °C; 6, 50 °C; 7, 55 °C; 8, 60 °C; 9, 65 °C. M = molecular markers. Electrophoretic images are representatives of three separate experiments.

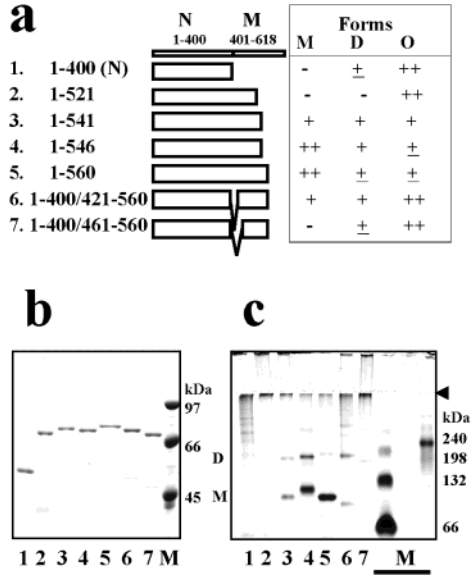

FIGURE 3: Oligomerization characteristics of the N domain tagged with the truncated M domain. (a) H_6HSP90α-N and that tagged with various truncated M domains, as shown schematically, were expressed. Purified proteins were electrophoresed on SDS−PAGE gel at a 7.5% polyacrylamide concentration (b) and a PAGE gel under nondenaturing conditions (c). The arrowhead at the right of panel c indicates the border between the concentration and separation gels. Numbers 1−7 in panels b and c correspond to those of panel a. M = molecular markers. States of recombinant proteins are summarized in panel a. M = monomer, D = dimer, and O = oligomer. Electrophoretic images are representatives of three separate experiments.

Suppression of the Oligomerization by the Intramolecular Interaction of Human HSP90α. It should be remembered that the full-length form of HSP90α exists as a dimer (see Figure 4c and refs *15* and *25*). Hence, it is reasonable to postulate that the potential activity of oligomerization of HSP90α-N is suppressed in the intact dimer. To test the role of the domain−domain interaction, we expressed the N domain of HSP90α attached to portions of the subsequent domain (Figure 3a,b). Polyacrylamide gel electrophoresis under nondenaturing conditions revealed that H_6HSP90α 1−521 and 1−400/461−560 predominantly existed as oligomers (Figure 3c, lanes 2 and 7). Monomeric, dimeric, and oligomeric forms were evenly present in H_6HSP90α 1−541 and 1−400/421−560 (lanes 3 and 6). To the contrary, the monomeric form was dominant in H_6HSP90α 1−546 (lane 4), and H_6HSP90α 1−560 was essentially monomeric (lane 5 and summarized in Figure 3a). It should be remembered that residues 401−541 could not, but 401−546 could, interact with the N domain, as described previously (*23*). Thus, the liberation of the N domain from the M domain triggered the self-oligomerization.

Minimal Region of the N Domain Responsible for Self-Oligomerization. Next we examined the minimal region of the N domain required for the oligomer formation. Initially, we compared two truncated forms of the N domain, i.e., H_6HSP90α 1−312 and 289−400. Because the expression of H_6HSP90α 289−400 was hardly detected with Coomassie staining (Figure 4b, left panel, lane 4), presumably because of the instability of small molecular exogenous proteins in *E. coli*, the entity was confirmed by immunoblotting with an anti-HSP90 mAb K41110 (*14*) (right panel, lane 4). PAGE under nondenaturing conditions clearly demonstrated that residues 289−400 existed as oligomers (Figure 4c, lane 4). In contrast, residues 1−312 migrated as a monomer (Figure 4b, lane 3). Thus, the oligomer-forming activity was specifically localized within residues 289−400.

To further define the minimal region responsible for oligomerization, we expressed a series of truncated forms (Figure 5a,b). Figure 5c clearly demonstrates that H_6HSP90α 1−312, 1−330, and 1−340 were monomeric and that H_6HSP90α 1−320 was a mixture of monomer and dimer. In contrast, H_6HSP90α 1−350 and further extended forms were oligomeric (Figure 5c, lanes 5−10, and summarized in Figure 5a).

To evaluate the N-terminal edge required for the oligomerization, we expressed residues 289−372 and 311−372 (Figure 6a). To express such small fragments stably in *E. coli*, they were expressed as GST fusion proteins. As shown in Figure 6b, both were highly oligomeric, indicating that residues from amino acid 311 to amino acid 372 were sufficient for the oligomerization. Taken together, our data indicate that residues 311−350 were sufficient for self-oligomerization and residues 341−350 were critical for it.

Amino Acids Essential within Residues 289−400 for the Interaction with the M Domain. The N domain of HSP90α can associate with the M domain of *E. coli* HtpG as well as it does with that of HSP90α (*12*). Thus, among residues 289−400, amino acids conserved among the HSP90-family members would appear to be important for this interaction. We selected 11 such amino acids and mutated them to Gly or Ala (Table 2). Bacterial two-hybrid analysis revealed that mutations of Trp297, Pro379, and Phe384 caused complete loss of the binding to the M domain and that mutations of

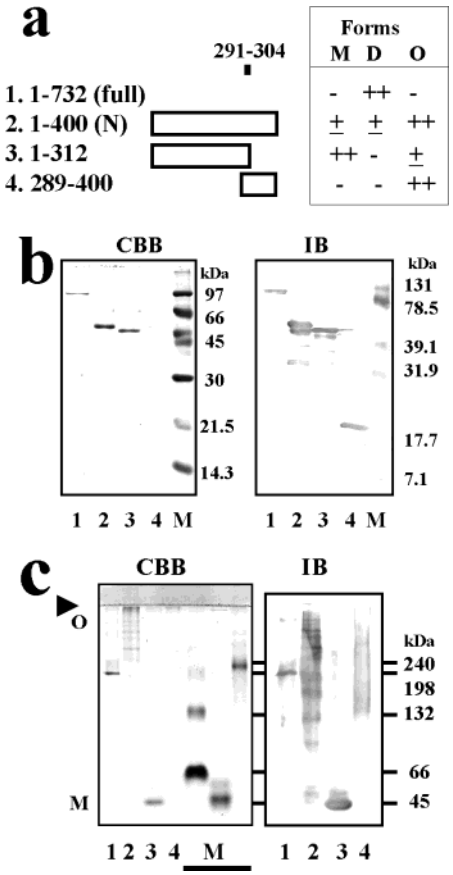

FIGURE 4: Oligomerization characteristics of truncated N domains. Various truncated N domains, shown schematically, were expressed (a). Residues 291−304 represent the epitope of K41110. H_6HSP90α (lane 1), H_6HSP90α-N (lane 2), H_6HSP90α 1−312 (lane 3), and H_6HSP90α 289−400 (lane 4) were electrophoresed on a SDS−PAGE gel (b) and on a PAGE gel under nondenaturing conditions (c). Proteins were visualized by Coomassie brilliant blue (CBB) staining or immunoblotting (IB) with K41110. The arrowhead in panel c indicates the border between the concentration and separation gels. Numbers 1−4 in panels b and c are in accord with those of panel a. M = molecular markers. States of recombinant proteins are summarized in panel a. M = monomer, D = dimer, and O = oligomer. Electrophoretic images are representatives of three separate experiments.

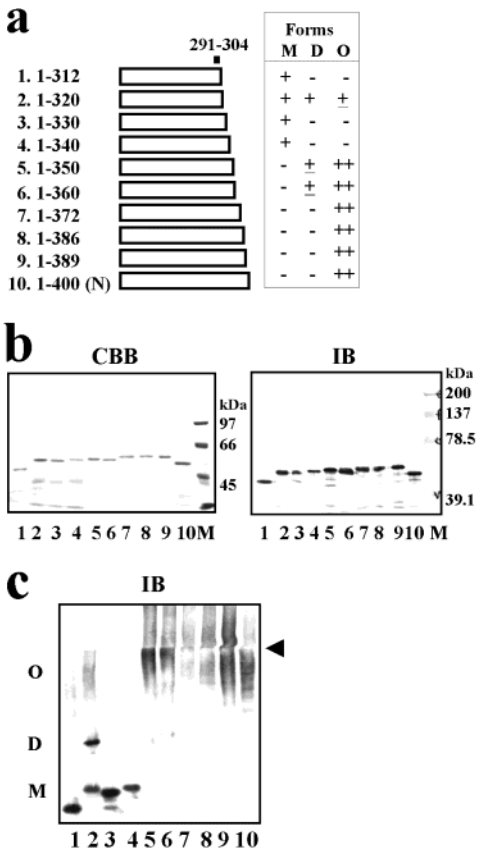

FIGURE 5: Region critical for the oligomerization. A series of forms of H_6HSP90α-N truncated at the C-terminus, shown schematically, were expressed (a). The amino acid number 291−304 on the top indicates the recognition site of K41110. Purified proteins separated on a 10% SDS−PAGE gel (b) and on a PAGE gel under nondenaturing conditions (c) were stained with CBB or by immunoblotting (IB). The arrowhead in panel c indicates the border between the concentration and separation gels. Numbers 1−10 in panels b and c are in accord with those of panel a. M = molecular markers. Molecular forms (M, monomer; D, dimer; and O, oligomer) of recombinant proteins are summarized in panel a. Electrophoretic images are representatives of three separate experiments.

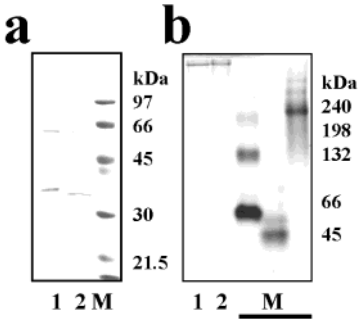

FIGURE 6: Oligomerization of GST-HSP90α 289−372 and 311−372. Purified forms of GST-HSP90α 289−372 (lane 1) and 311−372 (lane 2) were separated by SDS−PAGE (a) and PAGE under nondenaturing conditions (b). M = molecular markers. Proteins were stained with CBB. Electrophoretic images are representatives of three separate experiments.

the remaining ones had no effect. To investigate whether these three amino acids could be considered unique ones, we further introduced a random mutation at these positions. Positive transformants grew up with red colonies on plates containing maltose and a pH indicator. As a result, hydrophobic amino acids such as Ile, Phe, and Leu could partially (18.7−35.4%) substitute for Trp at position 297, and Met384 showed approximately one-half of the activity of Phe384 (Table 3). However, in three trials, one of which used primers carrying NNN at position Pro379 and two of which used primers carrying NSN at the position (N = G, A, T, or C and S = G or C), no colony encoding other than Pro379 was obtained, indicating that Pro379 was solely needed to be located at this position.

As shown in Table 2, four amino acids, i.e., Asp390, Leu396, Ser399, and Arg400, located near the C-terminal end of the N domain, were highly conserved but were dispensable for binding to the M domain. Thus, we supposed that the C-terminal end of the domain might be dispensable for the function. In fact, the C-terminal 11 amino acids were dispensable, but further 3 amino acid truncation disrupted the function (Table 4).

Limited Proteolysis of the N Domain. The present study strongly suggested that the client-binding site of HSP90α, experimentally monitored by the self-oligomerization, was localized within the N domain. However, there might be an

Table 2: Effect of Point Mutations in the N Domain on the Interaction with the M Domain[a]

pKT25[kan]-HSP90α 1−400	activity ± SD (%)
pKT25[kan]	7.8 ± 0.5
wt	100.0 ± 0.4
Asn291Gly	99.8 ± 0.1
Trp297Gly	9.4 ± 1.0
pKT25[kan]	10.4 ± 2.4
wt	100.0 ± 6.0
Leu363Ala	94.0 ± 19.2
Ile370Ala	109.2 ± 19.6
Pro379Ala	14.1 ± 3.3
Phe384Ala	12.5 ± 1.4
Gly387Ala	96.7 ± 17.6
Asp390Ala	113.8 ± 32.7
Leu396Ala	112.0 ± 20.6
Ser399Ala	96.5 ± 16.6
Arg400Ala	102.7 ± 6.6

[a] Binding activity of the N domain to the MC domain was set at 100%. Values are means ± SD of three independent colonies. Data are representatives of three separate experiments.

Table 3: Screening of Amino Acids at Positions of Trp297, Pro379, and Phe384 in the N Domain That Restore the Interaction with HSP90α-MC[a]

nucleotides	amino acid	activity ± SD (%)
TGG	Trp297	100 ± 5.3
ATT	Ile	35.4 ± 12.5
TTT	Phe	32.3 ± 20.1
TTT	Phe	28.0 ± 8.7
TTA	Leu	24.4 ± 7.5
ATT	Ile	22.9 ± 7.1
CTT	Leu	20.8 ± 8.8
TTT	Phe	19.6 ± 10.5
TTT	Phe	18.7 ± 6.7
AAT	Asn	17.9 ± 6.2
TAT	Tyr	12.0 ± 4.4
CCT	Pro379	100.0 ± 1.2
CCG	Pro	97.3 ± 8.1
CCC	Pro	105.0 ± 5.0
CCT	Pro	108.0 ± 1.3
TTC	Phe384	100.0 ± 7.1
TTT	Phe	78.8 ± 10.2
ATG	Met	57.8 ± 7.6
ATG	Met	54.5 ± 13.2
ATG	Met	44.7 ± 6.6
TTA	Leu	16.1 ± 5.0
vector		2.9 ± 1.6

[a] Binding activity of the N domain to the MC domain was set at 100%. Values are means ± SD of three or four independent colonies. Data are representatives of three separate experiments.

Table 4: Role of the C-Terminal Region of the N Domain on the Interaction with the MC Domain[a]

pKT25[kan]-HSP90α	activity ± SD (%)
pKT25[kan]	3.3 ± 1.5
1−400 (N)	100.0 ± 8.5
1−389	108.3 ± 2.6
1−386	4.9 ± 1.2
1−372	2.1 ± 0.5
1−320	3.7 ± 0.9

[a] Binding activity of the N domain to the MC domain was set at 100%. Values are means ± SD of three independent colonies. Data are representatives of two separate experiments.

alternative interpretation. That is, the bacterially expressed N domain of HSP90α might be misfolded and thereby aggregated. To test this possibility, we compared the molecular configuration of H_6HSP90α-N and H_6HSP90α by limited proteolysis.

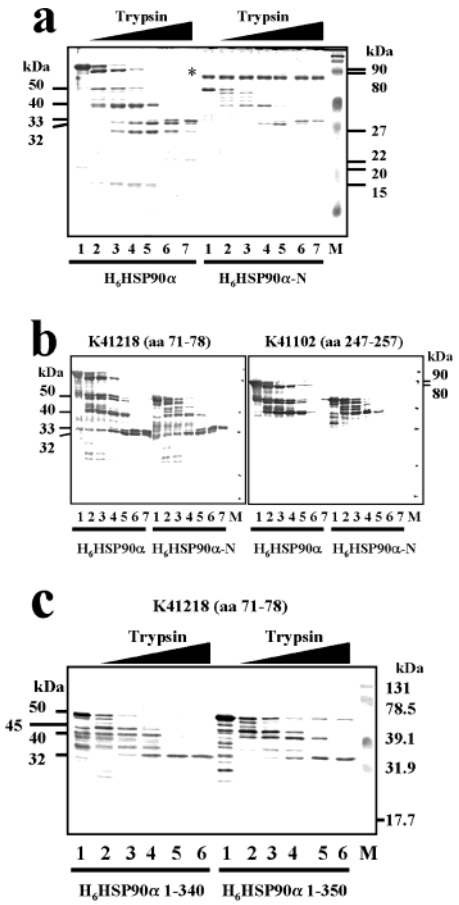

FIGURE 7: Limited proteolysis of recombinant proteins in oligomeric forms. (a, b) H_6HSP90α (40 μg/50 μL) or H_6HSP90α-N (22 μg/50 μL) supplemented with 18 μg of bovine albumin (shown by an asterisk) to adjust the total amount of proteins was incubated overnight at 30 °C without (lane 1) or with 0.001, 0.003, 0.01, 0.03, 0.1, and 0.3 μg (lanes 2−7) of trypsin that had been treated with N^{α}-acetyl-L-tosyl-L-phenylalanine chloromethyl ketone. Thereafter, aliquots (4 μg) of the samples were subjected to SDS−PAGE at a 15% polyacrylamide gel. Separated proteins were either stained with Coomassie brilliant blue (a) or subjected to immunoblotting with mAb K41218 (left) or K41102 (right) (b). Apparent molecular masses on the right represent the bands specific for proteolyzed H_6HSP90α, and those on the left represent the bands common in the two samples. In panel a, an asterisk indicates the position of bovine serum albumin. (c) H_6HSP90α 1−340 or 1−350 (6 μg/40 μL) was incubated without (lane 1) or with 0.001, 0.003, 0.01, 0.03, and 0.1 μg (lanes 2−6) of trypsin overnight at 30 °C. Thereafter, an aliquot (1 μg) was subjected to SDS−PAGE at a 15% polyacrylamide gel, followed by immunoblotting with K41218. M = kaleidoscope molecular markers. Electrophoretic images are representatives of two separate experiments.

All tryptic fragments of H_6HSP90α-N, i.e., 32-, 33-, and 40-kDa species, as well as 50-kDa H_6HSP90α-N itself (molecular masses represented on the left of Figure 7a), were also present in proteolyzed H_6HSP90α and were recognized by both K41218 and K41102 (Figure 7b). The 32- and 33-kDa species, which were recognized by K41218, but not with K41102, should contain the N-terminal ATP-binding domain (residues 1−220/230) but lost the highly charged region (residues 223−289) (*14*, *17*), The remaining 15-, 20-, 22-, and 27-kDa fragments (indicated on the right of Figure 7a) specific for digestion of H_6HSP90α should be derived from the MC domain, and actually, they were not recognized by

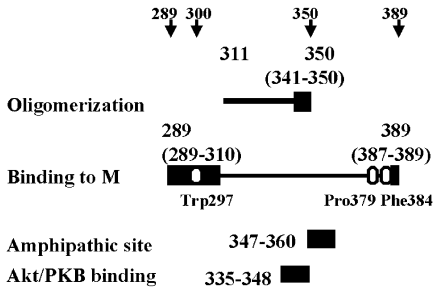

FIGURE 8: Regions of human HSP90α required for the self-oligomerization/client binding and association with the M domain. Residues 311−350 are sufficient for self-oligomerization, and residues 341−350 are critical. Residues 289−389 are sufficient for the binding to the M domain, and residues 289−310 (*23*) and residues 387−389 as well as Trp297, Pro379, and Phe384 are critical. Residues 347−360 constitute an amphipathic segment proposed to interact with client proteins (*7*); and 335−348, a region essential for the binding to Akt/PKB (*6*).

the mAbs (Figure 7b). The 80-kDa species corresponded to the NM domain (*14*). Additionally, it should be noted that the trypsin concentrations required for the production of these fragments were comparable between the two proteins.

Because the transition from the monomer to the oligomer was critical between H_6HSP90α 1−340 and 1−350 (Figure 5c), they were also subjected to the limited proteolysis. Again, the cleavage patterns were indistinguishable between monomeric and oligomeric forms (Figure 7c). Taken together, we concluded that the molecular configuration of H_6-HSP90α-N was indistinguishable from that of the full-length form and the same was true for H_6HSP90α 1−340 and 1−350, indicating that the oligomerization was not caused by misfolding of the N domain but induced by exposure of the client-binding site of the domain.

DISCUSSION

On the basis of the three-dimensional structure of residues 273−516, Beyer et al. (*7*) recently proposed that an amphipathic segment of yeast HSP82, residues Ala327−Asn340, equivalent to Ala347−Asn360 of human HSP90α, forms a potential client-binding site. With the study on HSP90β in mind (*6*), they proposed that amino acids 327−340 of yeast HSP82, equivalent to residues 335−348 of human HSP90α, are essential for the binding to serine/threonine kinase Akt/PKB. However, the amphipathic region scarcely overlaps with the latter region (Figure 8). Moreover, the amphipathic region is less conserved among the members of the HSP90-family protein. Notably, the present study demonstrated that residues 311−350 are sufficient for the oligomerization, and our results further demonstrated that residues 341−350 are critical for self-oligomerization of HSP90α. We recently demonstrated that residues 289−400 are also important for the binding to neuropeptide Y (*26*). Therefore, residues 311−350, being located adjacent to the highly immunogenic site (residues 291−304) of human HSP90α (*14*), seem to directly associate with client proteins, such as neuropeptide Y and Akt/PKB. Interestingly, we recently reported that the electron microscopic image of the mAb K3720 (recognizing at residues 291−304) attached HSP90 dimer was indistinguishable to that of the HSP90 dimer bound to neuropeptide Y bridged to streptavidin (*26*). Moreover, it should be noted that residues 341−350, which are critical for the self-oligomerization of the N domain, completely overlap the region (residues 335−348) essential for the interaction with Akt/PKB (Figure 8).

One might make the criticism that truncated forms of HSP90 expressed in the present study might simply form aggregates or inclusion bodies, because recombinant proteins expressed in *E. coli*, especially truncated forms of proteins, tend to form such products. However, the present observations on the N domain make this an unlikely possibility. That is, (i) the oligomeric form was essentially soluble on centrifugation at 30000*g* for 0.5 h; (ii) an analysis by limited proteolysis indicated the molecular configuration of the oligomerized form to be indistinguishable to the other forms, such as the N domain of the full-length protein (Figure 7); (iii) the oligomer formation of the N domain tightly correlated with the separation of N from the M domain (Figure 3b); (iv) as discussed above, the region critical for the self-oligomerization exactly corresponded to that essential for the binding to Akt/PKB; (v) finally, we should note that the self-oligomerization of truncated forms of human HSP90 did not specifically occur in the bacterial expression system, but the truncated form of HSP90 seems to be self-oligomerized in eukaryotic cells as discussed below (*3*, *27*).

Binart et al. (*3*) and Cadepond et al. (*27*) developed a coexpression system of HSP90 and the steroid receptors in baculovirus-infected Sf9 cells: two truncated forms of chick HSP90α that did not possess the residues equivalent to residues 396−423 and 534−585 of human HSP90α formed abnormally large heteromeric complexes with the glucocorticoid receptor, and the receptor in the complex could not bind its hormone. Keeping our results (Figure 3 and ref *14*) in mind, the two truncated forms did not have the residues equivalent to amino acids 401−423 or 534−546 of human HSP90α essential for the interaction with the N domain, and therefore they were likely to form abnormally large oligomers, as the bacterially expressed N domain did. It is not surprising that the large complex was not functional, because HSP90 carrying the mutated M domain that could not bind to the N domain was not functional in yeast (*23*). Hence, their observation further supports the notion that the oligomer formation of the N domain is an intrinsic property in mammalian HSP90.

The mechanism on self-oligomerization of the HSP90 molecular chaperone observed in the present study is akin to the heat-induced activation of the client-binding activity proposed previously for *E. coli* HtpG (*12*). We therefore propose a common mechanism on client binding of the HSP90-family proteins: The client-binding site of the N domain is generally concealed by the association with the M suppressor domain, and the molecular chaperone activity emerges at elevated temperatures by disruption of this interaction. Our results indicate that the client-binding site occupies a restricted region (residues 311−350 and, particularly, residues ∼341−350) of residues 289−389 required for the interaction with the M domain (Figure 8). In an intact HSP90 dimer, a pair of the client-binding sites may clamp a target protein as proposed (*28*−*30*) through the dimeric interaction at the C-terminal 191 amino acids (*15*). Our present and previous studies (*31*) strongly suggest that the domain topology of the HSP90 dimer in the client-unbound state is considerably different from the bound one.

ACKNOWLEDGMENT

We greatly acknowledge Drs. H. Iwanari and H. Yamashita (Institute of Immunology Co., Tochigi, Japan) for the preparation of anti-HSP90 mAbs.

REFERENCES

1. Yonehara, M., Minami, Y., Kawata, Y., Nagai, J., and Yahara, I. (1996) Heat-induced chaperone activity of HSP90, *J. Biol. Chem. 271*, 2641−2645.
2. Nemoto, T. K., Ono, T., and Tanaka, K. (2001) Substrate-binding characteristics of proteins in the 90 kDa heat shock protein family, *Biochem. J. 354*, 663−670.
3. Binart, N., Lombes, M., and Baulieu, E.-E. (1995) Distinct functions of the 90 kDa heat shock protein (hsp90) in oestrogen and mineralocorticoid receptor activity: effects of hsp90 deletion mutants, *Biochem. J. 311*, 797−804.
4. Miyata, Y., and Yahara, I. (1995) Interaction between casein kinase II and the 90-kDa stress protein, *Biochemistry 34*, 8123−8129.
5. Louvion, J. F., Warth, R., and Picard, D. (1996) Two eukaryotic-specific regions of Hsp82 are dispensable for its viability and signal transduction functions in yeast, *Proc. Natl. Acad. Sci. U.S.A. 93*, 13937−13942.
6. Sato, S., Fujita, N., and Tsurui, T. (2000) Modulation of Akt kinase activity by binding to Hsp90, *Proc. Natl. Acad. Sci. U.S.A. 97*, 10832−10837.
7. Meyer, P., Prodromou, C., Hu, B., Vaughan, C., Roe, S. M., Panaretou, B., Piper, P. W., and Pearl, L. H. (2003) Structural and functional analysis of the M segment of Hsp90: implications for ATP hydrolysis and client protein cochaperone interactions, *Mol. Cell 11*, 647−658.
8. Young, J. C., Schneider, C., and Hartl, F. U. (1997) *In vitro* evidence that hsp90 contains two independent chaperone sites, *FEBS Lett. 418*, 139−143.
9. Scheibel, T., Weikl, T., and Buchner, J. (1998) Two chaperone sites in Hsp90 differing in substrate specificity and ATP dependence, *Proc. Natl. Acad. Sci. U.S.A. 95*, 1495−1499.
10. Minami, M., Nakamura, M., Yasuhumi, E., and Minami, Y. (2001) Both the N- and C-terminal chaperone sites of Hsp90 participate in protein folding, *Eur. J. Biochem. 268*, 2520−2524.
11. Roher, N., Miro, F., Boldyreff, B., Llorens, F., Plana, M., Issinger, O.-G., and Itarte, E. (2001) The C-terminal domain of human grp94 protects the catalytic subunit of protein kinase CK2 (CK2α) against thermal aggregation: role of disulfide bonds, *Eur. J. Biochem. 268*, 429−436.
12. Tanaka, E., Nemoto, T. K., and Ono, T. (2001) Liberation of the intramoleular interaction as the mechanism of heat-induced activation of HSP90 molecular chaperone, *Eur. J. Biochem. 268*, 5270−5277.
13. Yamada, S., Ono, T., Mizuno, A., and Nemoto, T. K. (2003) A hydrophobic segment within the C-terminal domain is essential for both client-binding and dimer formation of the HSP90-family molecular chaperone, *Eur. J. Biochem. 270*, 146−154.
14. Nemoto, T., Sato, N., Iwanari, H., Yamashita, H., and Takagi T. (1997) Domain structures and immunogenic regions of the 90-kDa heat-shock protein (HSP90): probing with a library of anti-HSP90 monoclonal antibodies and limited proteolysis, *J. Biol. Chem. 272*, 26179−26187.
15. Nemoto, T., Ohara-Nemoto, Y., Ota, M., Takagi, T., and Yokoyama, K. (1995) Mechanism of dimer formation of the 90-kDa heat-shock protein, *Eur. J. Biochem. 233*, 1−8.
16. Nemoto, T. K., Ono, T., Kobayakawa, T., Tanaka, E., Baba, T. T., Tanaka, K., Takagi, T., and Gotoh, T. (2001) Domain-domain interactions of HtpG, an *Escherichia coli* homologue of eukaryotic HSP90 molecular chaperone, *Eur. J. Biochem. 268*, 5258−5269.
17. Stebbins, C. E., Russo, A. A., Schneider, C., Rosen, N., Hartl, F. U., and Pavletich, N. P. (1997) Crystal structure of an Hsp90-geldanamycin complex: targeting of a protein chaperone by an antitumor agent, *Cell 89*, 239−250.
18. Prodromou, C., Roe, S. M., O'Brien, R., Ladbury, J. E., Piper, P. W., and Pearl, L. H. (1997) Identification and structural characterization of the ATP/ADP-binding site in the Hsp90 molecular chaperone, *Cell 90*, 65−75.
19. Yamazaki, M., Tashiro, H., Yokoyama, K., and Soeda, E. (1990) Molecular cloning of cDNA encoding a human heat-shock protein whose expression is induced by adenovirus type 12 E1A in HeLa cells, *Agric. Biol. Chem. 54*, 3163−3170.
20. Bardwell, J. C. A., and Craig, E. A. (1987) Eukaryotic M_r 83,000 heat shock protein has a homologue in *Escherichia coli*, *Proc. Natl. Acad. Sci. U.S.A. 84*, 5177−5181.
21. Nemoto, T., Matsusaka, T., Ota, M., Takagi, T., Collinge, D. B., and Walther-Larsen, H. (1996) Dimerization characteristics of the 94-kDa glucose-regulated protein, *J. Biochem. 120*, 249−256.
22. Karimova, G., Ullmann, A., and Ladant, D. (2001) Protein−protein interactions between *Bacillus stearothernophilus* tyrosyl-tRNA-synthase subdomains revealed by a bacterial two-hybrid system, *J. Mol. Microbiol. Biotechnol. 3*, 73−82.
23. Matsumoto, S., Tanaka, S., Nemoto, T., K., Ono, T., Kobayakawa, T., Takagi, T., Imai, J., Kimura, Y., Yahara, I., Yamada S., Ayuse, T., Oi, K., and Mizuno, A. (2002) Interaction between the N-terminal and middle regions is essential for the in vivo function of HSP90 molecular chaperone, *J. Biol. Chem. 277*, 34959−34966.
24. Welch, J. W., and Feramisco, J. R. (1982) Purification of major heat shock proteins, *J. Biol. Chem. 257*, 14949−14959.
25. Minami, Y., Kawasaki, H., Miyata, Y., Suzuki, K., and Yahara, I. (1991) Analysis of native forms and their isoform compositions of the mouse 90-kDa heat-shock protein, HSP90, *J. Biol. Chem. 266*, 10099−10103.
26. Ishiwatari-Hayasaka, H., Maruya, M., Nemoto, T. K., Sreedhar, A. S., Csermely, P., and Yahara, I. (2003) Interaction of neuropeptide Y and Hsp90 through a novel peptide binding region, *Biochemistry 42*, 12972−12980.
27. Cadepond, F., Binart, N., Chambraud, B., Jibard, N., Schweizer-Groyer, G., Segard-Maurel, I., and Baulieu, E. E. (1993) Interaction of glucocorticoid receptor and wild-type or mutated 90-kDa heat shock protein coexpressed in baculovirus-infected Sf9 cells, *Proc. Natl. Acad. Sci. U.S.A. 90*, 10434−10348.
28. Prodromou, C., Panaretou, B., Chohan, S., Siligardi, G., O'Brien, R., Ladbury, J. E., Roe, S. M., Piper, P. W., and Pearl, L. H. (2000) The ATPase cycle of Hsp90 drives a molecular 'clamp' via transient dimerization of the N-terminal domains, *EMBO J. 16*, 4383−4392.
29. Prodromou, C., Roe, S. M., Piper, P. W., and Pearl, L. H. (1997) A molecular clamp in the crystal structure of the N-terminal domain of the yeast Hsp90 chaperone, *Nat. Struct. Biol. 4*, 477−482.
30. Pearl, L. H., and Prodromou, C. (2000) Structure and in vivo function of Hsp90, *Curr. Opin. Struct. Biol. 10*, 46−61.
31. Maruya, M., Sameshima, M., Nemoto, T., and Yahara, I. (1999) Monomer arrangement in HSP90 dimer as determined by decoration with N- and C-terminal specific antibodies, *J. Mol. Biol. 285*, 903−907.

BI036235F